Journal of Medicinal Chemistry

ARTICLE

pubs.acs.org/jmc

7-Azaindenoisoquinolines as Topoisomerase I Inhibitors and Potential Anticancer Agents

Evgeny Kiselev,[†] Sean DeGuire,[†] Andrew Morrell,[†] Keli Agama,[‡] Thomas S. Dexheimer,[‡] Yves Pommier,[‡] and Mark Cushman*[,†]

[†]Department of Medicinal Chemistry and Molecular Pharmacology, College of Pharmacy, and The Purdue Center for Cancer Research, Purdue University, West Lafayette, Indiana, 47907, United States

[‡]Laboratory of Molecular Pharmacology, Center for Cancer Research, National Cancer Institute, Bethesda, Maryland 20892-4255, United States

ABSTRACT: A series of 7-azaindenoisoquinoline topoisomerase I (Top1) inhibitors have been prepared to investigate the effect of increased electron affinity of the aromatic system on the ability to stabilize the Top1−DNA cleavage complex. Ab initio calculations suggest that introduction of nitrogen into the aromatic system of the indenoisoquinolines would facilitate charge transfer complex formation with DNA, thus improving the $\pi-\pi$ stacking interactions. The present study shows that 7-azaindenoisoquinolines demonstrate improved water solubility without any decrease in Top1 inhibitory activity or cytotoxicity. Analysis of the biological results reveals that smaller lactam ring substituents enable intercalation into both free DNA and Top1−DNA cleavage complex, whereas larger substituents only allow binding to the cleavage complex but not free DNA. Free DNA binding suppresses Top1-catalyzed DNA cleavage at high drug concentrations, whereas DNA cleavage and inhibition of religation occurs at low drug concentration.

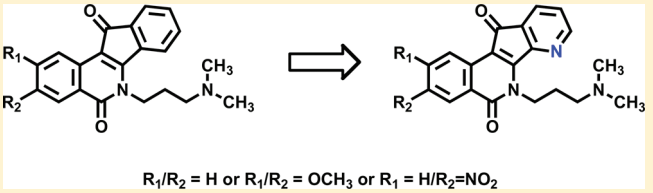

INTRODUCTION

Human topoisomerase type I (Top1) is a ubiquitous cellular enzyme. It is a member of the topoisomerase family of enzymes that solve DNA topological problems associated with supercoiling.[1,2] DNA supercoiling occurs during a number of vital cellular processes such as replication, transcription, and DNA repair. Top1 relaxes DNA by producing reversible single-strand DNA cuts. The generally accepted mechanism of Top1 action involves formation of a covalent link between the catalytic tyrosine 723 residue of Top1 and the 3′-end of the cut DNA strand in the Top1−DNA cleavage complex (Top1-DNAcc). The rotation of the 5′-end around the intact strand allows for relaxation of the supercoils.[3] Once the tension caused by supercoiling has been removed, the backbone of the cut strand is religated and Top1 released. This mechanism has been substantiated by crystallography of a stable form of the Top1-DNAcc.[4]

The dependency of living organisms on topoisomerases in processes like DNA replication during cell division has made topoisomerases attractive drug targets for anticancer chemotherapy. The search for Top1 inhibitors was eventually rewarded with the isolation of camptothecin (**1**) in 1966 from an extract of the Chinese tree *Camptotheca acuminata* (Figure 1).[5] It was found that **1** was capable of inducing DNA cleavage in the presence of Top1. The ability of **1** to bind to and stabilize the Top1-DNAcc by forming a drug−Top1−DNA ternary complex lies at the heart of its mechanism of action. Further development of **1** as an anticancer drug was hindered by its poor water solubility.[6] Screening of a number of synthetic analogues of **1** led to the clinically used Top1 inhibitors, topotecan and irinotecan, which possess basic functionality and thus improved water solubility and bioavailability. Unfortunately, the derivatives of **1** have limitations in their clinical use. The lactone form is in equilibrium with its carboxylate form at physiological pH, which has reduced bioavailability due to plasma protein binding. Additionally, the treatment with derivatives of **1** requires long infusion times due to quick reversibility of the Top1-DNAcc.[1,2]

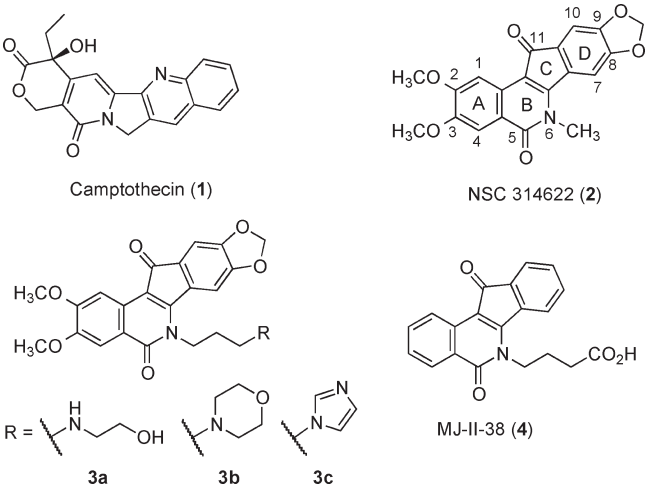

Figure 1. Representative Top1 inhibitors.

Received: June 6, 2011
Published: August 08, 2011

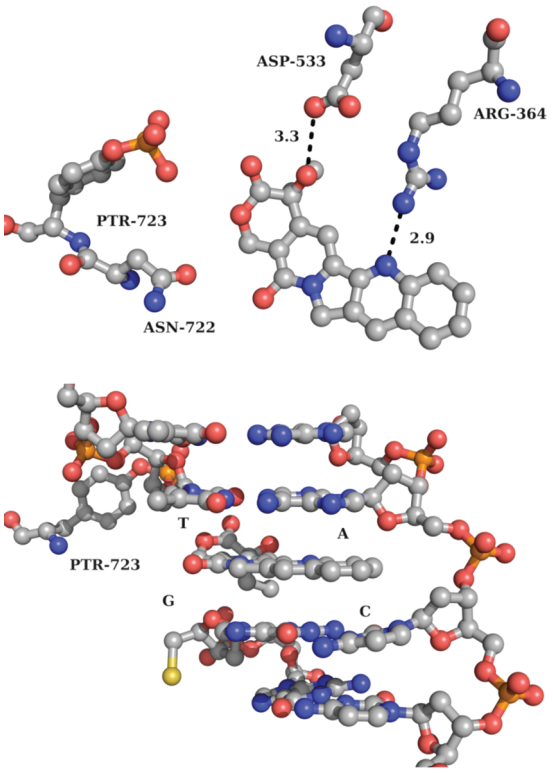

Figure 2. Binding mode of **1** within **1**—Top1—DNA ternary complex: hydrogen bonds to Top1 residues (top) and $\pi-\pi$ stacking with flanking DNA base pairs (bottom). The sulfur atom originated from the phosphorothiolate duplex oligonucleotide substrate used in the crystallography studies.[7]

Crystallography of the **1**—Top1—DNA ternary complex revealed that **1** is capable of stabilizing the Top1-DNAcc by binding to it at the site of cleavage.[7] The described binding mode showed an extended region of $\pi-\pi$ stacking between the polycyclic core of **1** and the DNA base pairs, as well as a number of polar interactions formed between **1** and Top1 residues (Figure 2). The intercalation of **1** into the Top1-DNAcc increases the distance between ends of the broken DNA strand and prevents religation, resulting in prolonged covalent attachment of Top1 to the DNA.

A new class of Top1 inhibitors, the indenoisoquinolines, emerged with the isolation of **2** (NSC 314622) as a byproduct of nitidine chloride synthesis (Figure 1).[8,9] A COMPARE analysis revealed similar cytotoxicity profiles between **1** and **2**.[10] However, observed differences in DNA cleavage site specificity between camptothecins and indenoisoquinolines suggested that different genes might be targeted more specifically with indenoisoquinolines.[6] Also and in contrast to **1**, the Top1-DNAcc trapped by **2** was more persistent in both cell- and enzyme-based assays.[6] Moreover, a structural comparison of the indenoisoquinolines and the camptothecins suggested that indenoisoquinolines would likely have enhanced chemical stability relative to that of the camptothecins. Further structure optimization of **2** and biological assessment of synthesized analogues led to the discovery of a number of potent Top1 inhibitors [e.g., MJ-III-65 (**3a**), NSC 724998 (NSC 743400, LMP400, **3b**), and NSC 725776 (LMP776, **3c**), Figure 1].[11,12] The morpholinopropyl and imidazolylpropyl analogues **3b** and **3c**[13,14] have been promoted to phase I clinical trials at National Cancer Institute.[15]

Scheme 1

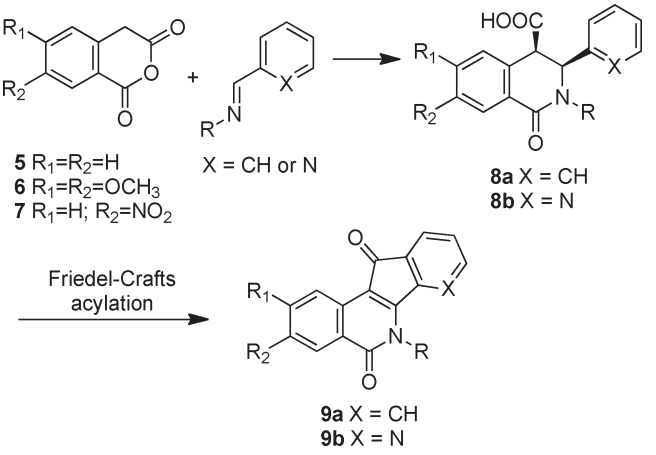

Replacement of the methyl group on the lactam B-ring of **2** with aminoalkyl chains was found to improve Top1 inhibitory activity and cytotoxicity of indenoisoquinolines.[16—18] Evaluation of a number of analogues with diverse substituents on the A- and D-rings also improved the anticancer properties of the indenoisoquinolines.[11,19] In particular, the most studied substituents on the D-ring were the electron-donating alkoxy groups. Only a very limited number of electron-withdrawing groups on the D-ring have been evaluated.[20] The present report describes a series of indenoisoquinolines containing an electron-deficient pyridine D-ring.

The goal of this project was to investigate the abilities of indenoisoquinolines to form charge-transfer complexes and to correlate this with their inhibitory potencies against Top1 by preparing and evaluating a series of 7-azaindenoisoquinoline derivatives, the 5*H*-pyrido[3′,2′:4,5]cyclopenta[1,2-*c*]isoquinoline-5-11(6*H*)-diones (Schemes 1 and 2). One approach to the modulation of the electron-attracting abilities of the indenoisoquinolines was to incorporate additional nitrogen atoms in the heterocyclic ring system itself. The incorporation of nitrogen into an aromatic ring system would be expected to increase electron affinity.[21] Thus, indenoisoquinolines containing additional nitrogen atoms should have greater capacities for charge-transfer complex formation with neighboring bases in the ternary complex.

CHEMISTRY

To date, the most frequently used synthetic approach to various indenoisoquinolines substituted on the indenone D-ring has been the condensation of homophthalic anhydrides (e.g., **5**—**7**, Scheme 1) with various Schiff bases, followed by cyclization of the resulting *cis*-isoquinolonic acids **8a** into indenoisoquinolinediones **9a** via intramolecular acylation, forming the central C-ring.[8,9,16—18]

In the case of 7-azaindenoisoquinolines **9b**, a 2-pyridyl Schiff base would have to be used as a precursor for the D-ring of a new molecule. Because of extremely low reactivity of pyridines in reactions of electrophilic aromatic substitution, cyclization of **8b** into **9b** would be very difficult (Scheme 1). Therefore, an alternative protocol has been followed.[22] According to this pathway, the commercially available 2-cyano-3-picoline **10** was treated with *N*-bromosuccinimide (NBS) in refluxing 1,2-dichloroethane in the presence of the radical initiator AIBN. Crude bromide **11** was subsequently treated with homophthalic anhydride (**5**), 4,5-dimethoxyhomophthalic anhydride (**6**),[23] or

dx.doi.org/10.1021/jm200719v |*J. Med. Chem.* 2011, 54, 6106–6116

Scheme 2[a]

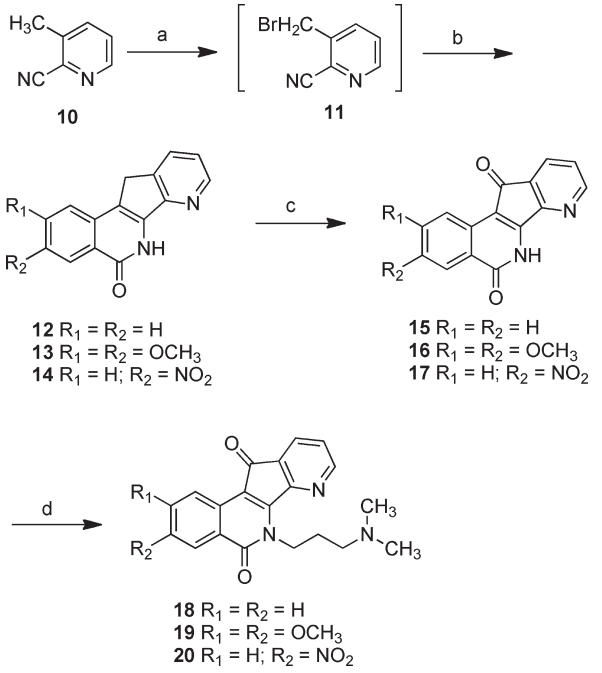

[a] Reagents and conditions: (a) NBS, AIBN, 1,2-dichloroethane, reflux, 2 h; (b) **5** (for **12**), **6** (for **13**) or **7** (for **14**), triethylamine, acetonitrile, reflux 10 h (**12** 31%, **13** 39%, **14** 12%); (c) selenium dioxide, 1,4-dioxane, reflux 16 h (**15** 89%, **16** 26%, **14** 59%); (d) DIAD, triphenylphosphine, 3-dimethylamino-1-propanol, THF, 23 °C, 3 days (**18** 59%, **19** 76%, **20** 62%).

4-nitrohomophthalic anhydride (**7**)[24] to provide **12**, **13**, or **14**, respectively (Scheme 2). Treatment of **12**−**14** with selenium dioxide in refluxing 1,4-dioxane provided indenoisoquinolines **15**−**17**.

It was previously shown that addition of the aminoalkyl chain to the sixth position of the indenoisoquinolines increases Top1 inhibitory activity.[11] Treatment of compounds **15**, **16**, and **17** with 3-dimethylamino-1-propanol, triphenylphosphine, and DIAD in tetrahydrofuran (Mitsunobu reaction) yielded compounds **18**, **19**, and **20** (Scheme 2). The overall yields for the syntheses of **18**, **19**, and **20** are modest at best (4−16% from **10**) but are comparable to those that could be achieved for most indenoisoquinoline systems via the Schiff base/homophthalic anhydride condensation and Friedel−Crafts acylation sequence (7−20% from benzaldehydes).[11]

A number of analogues of **2** with the lactam nitrogen bearing various aminopropyl substituents were previously prepared and evaluated as Top1 inhibitors and antiproliferative agents.[11,16−18] Use of such substituents as aminopropyl, ethanolaminopropyl, morpholinopropyl, and imidazolylpropyl was shown to improve both cytotoxicity and inhibitory potency of indenoisoquinolines. The optimization of the aminopropyl group ultimately led to the identification of **3b** and **3c** that were advanced to clinical trials.[15] It was our intention to explore these aminopropyl substituents in the context of the 7-azaindenoisoquinoline system. For this purpose Mitsunobu reaction with 4-(3-hydroxypropyl)morpholine was used in order to prepare morpholinopropyl analogues **21**−**23** (Scheme 3). Compounds **19** and **20** were also prepared in an alternative two-step sequence. Treatment of **15** and **16** with excess of 1,3-dibromopropane in the presence of sodium hydride,

Scheme 3[a]

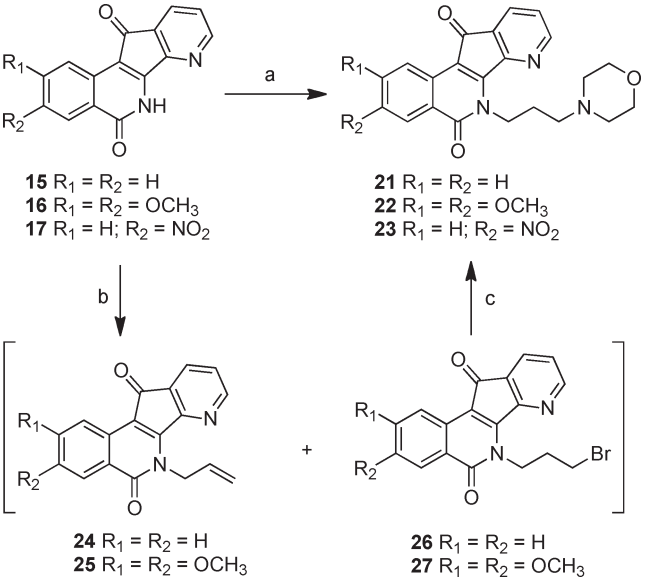

[a] Reagents and conditions: (a) DIAD, triphenylphosphine, 4-(3-hydroxypropyl)morpholine, THF, 23 °C, 3 days (**21** 62%, **22** 68%, **23** 30%); (b) NaH, DMF, −5 to 23 °C, 3 h, 1,3-dibromopropane, −5 to 23 °C, 12 h; (c) morpholine, 1,4-dioxane, reflux, 6 h (**21** 15%, **22** 17%, **24** 13−50%, **25** 21−35%).

Scheme 4[a]

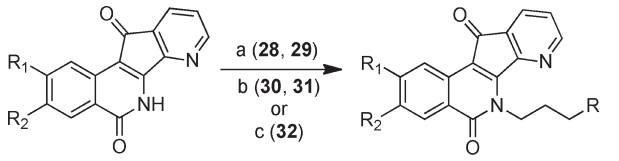

[a] Reagents and conditions: (a) (1) NaH, DMF, −5 to 23 °C, 3 h, 1,3-dibromopropane, −5 to 23 °C, 12 h, (2) imidazole, 1,4-dioxane, reflux, 6 h (**28** 17%, **29** 17%); (b) (1) NaH, DMF, −5 to 23 °C, 3 h, 1,3-dibromopropane, −5 to 23 °C, 12 h, (2) 2-ethanolamine, 1,4-dioxane, reflux, 6 h (**30** 16%, **31** 20%); (c) (1) NaH, DMF, −5 to 23 °C, 3 h, 1,3-dibromopropane, −5 to 23 °C, 12 h, (2) NaN_3, DMF, 23 °C, 12 h; (3) $P(OC_2H_5)_3$, benzene, reflux, 6 h; (4) HCl, H_2O, reflux, 3 h (**32** 18%).

followed by reaction with morpholine, yielded **21** and **22**, respectively. Allyl-substituted indenoisoquinolines **24** and **25** were isolated as minor products along with their morpholinopropyl analogues **21** and **22**. It was noticed that the chromatographic separation of the allyl analogues **24** and **25** was much easier after the intermediate bromides **26** and **27** were converted to corresponding morpholine analogues **21** and **22**. Therefore, the conversion of **15** and **16** into their respective aminopropyl derivatives was carried out without isolation of the intermediate bromides **26** and **27**.

The second approach also provides an easy access to the aminoalkyl analogues that are difficult to obtain via Mitsunobu reaction because of the presence of multiple hydroxyl or amino groups or commercial unavailability of the starting amino alcohols.

dx.doi.org/10.1021/jm200719v |J. Med. Chem. 2011, 54, 6106–6116

Table 1. Top1 Inhibitory and Antiproliferative Activity of 7-Azaindenoisoquinolines

		cytotoxicity GI_{50}, μM[c]								
			lung	colon	CNS	melanoma	ovarian	renal	prostate	breast
compd	Top1 cleavage[a]	MGM[b]	HOP-62	HCT-116	SF-539	UACC-62	OVCAR-3	SN12C	DU-145	MCF7
1	++++	0.04	0.01	0.03	0.01	0.01	0.22	0.02	0.01	0.013
2	++	8.51	2.82	11.48	1.66	0.56	22.39	25.70	4.79	1.91
18	+++	1.78	1.51	0.41	1.91	2.69	2.57	0.81	1.35	0.25
19	+++	4.50	3.392	1.58	4.07	13.18	3.55	3.16	1.70	0.44
20	+++(+)	1.86	2.349	0.44	2.69	3.31	2.29	1.0	0.93	0.36
21	+(+)	15.49	35.48	1.86	5.62	>100	28.18	5.37	3.55	2.75
22	++	0.30	0.30	0.22	0.29	0.095	0.37	0.52	0.31	0.052
23	+++									
28	++	7.24	7.24	1.20	5.13	35.48	8.71	3.72	2.88	3.39
29	++									
30	+	1.29	1.41	0.30	0.87	3.09	1.55	0.76	0.41	0.48
31	+(+)	0.29	0.30	0.15	0.26	0.12	0.34	0.23	0.32	0.074
32	+(+)	2.09	3.02	0.38	2.19	8.13	1.58	2.88	1.62	49
33	+++	1.86	1.74	0.58	1.86	0.51	1.66	0.91	1.32	0.55
34	++(+)	6.17	11.48	2.45	6.17	6.61	5.89	10.96	4.47	6.17
35	+++	9.77	5.62	6.46		7.08	32.36	4.17	5.62	0.24

[a] The relative Top1 inhibitory potencies of the compounds are presented as follows: 0, no detectable activity; +, weak activity; ++, activity similar to that of **2**; +++ and ++++, greater activity than that of **2**; ++++, activity similar to that of 1 μM **1**. [b] Mean graph midpoint for growth inhibition of all human cancer cell lines successfully tested. [c] The cytotoxicity GI_{50} values listed are the concentrations corresponding to 50% growth inhibition and are the result of single determinations.

Examples of such analogues **28**−**32** are presented in Scheme 4. According to this method, reaction of intermediate bromides **26** and **27** with imidazole yielded **28** and **29**, respectively. Similarly, ethanolamine analogues **30** and **31** were isolated after reaction of **26** and **27** with 2-ethanolamine. The reaction of **27** with sodium azide followed by treatment with triethyl phosphite yielded amine **32**.

BIOLOGICAL RESULTS AND DISCUSSION

All of the target compounds were tested for induction of DNA damage in Top1-mediated DNA cleavage assays.[25] For this purpose, a ^{32}P 3′-end-labeled 117-bp DNA fragment was incubated with human recombinant Top1 and increasing concentration of a tested compound. The DNA fragments were separated on a denaturing gel. The Top1 inhibitory activity was assigned based on the visual inspection of the number and intensities of the DNA cleavage bands and expressed in semiquantitative fashion relative to the Top1 inhibitory activities of compounds **1** and **2**: 0, no detectable activity; +, weak activity; ++, activity similar to that of **2**; +++, activity greater than that of **2**; ++++, equipotent to **1** (Table 1).

The antiproliferative activity of each compound was determined in the National Cancer Institute (NCI) screen.[26−29] Cells of approximately 60 different human cancer cell lines were incubated for 48 h with five 10-fold dilutions of the tested compounds starting from 100 μM and then treated with sulforhodamine B dye. The ratios of recorded optical densities relative to that of the control were plotted as a function of the common logarithm of the tested compound concentrations. The interpolation between the points located above and below the 50% percentage growth provided respective 50% growth inhibition (GI_{50}) values. The GI_{50} and the mean graph midpoint (MGM)

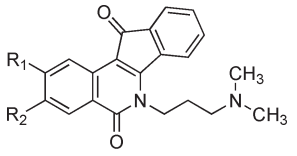

33 $R_1 = R_2 = H$
34 $R_1 = R_2 = OCH_3$
35 $R_1 = H$; $R_2 = NO_2$

Figure 3. Representative indenoisoquinolines.

values of the prepared indenoisoquinolines in selected cell lines are presented in Table 1.

The Top1 inhibitory activities were compared to the previously prepared indenoisoquinolines **33**−**35** (Figure 3).[30] The results clearly show that azaindenoisoquinolines **18**−**20** are equipotent or more potent against Top1 than corresponding indenoisoquinolines **33**−**35** (Table 1). A preservation of the level of cytotoxicity in the 7-azaindenoisoquinoline compounds was also observed relative to the corresponding indenoisoquinolines **33**−**35**. A slight increase in cytotoxicity was observed in ethanolaminopropyl **30**, **31**, and aminopropyl **32** analogues. Interestingly, the increase in cytotoxicity coincided with the decrease of Top1 activity and suggested an additional mechanism of action responsible for the increased cytotoxicity.

In some cases, the intensities of the cleavage bands were reduced at the highest tested concentration of the drug, 100 μM. This result can be attributed to the ability of these indenoisoquinolines to intercalate into free DNA, preventing DNA cleavage by Top1. Interestingly, when analogues **19**, **22**, **29**, **31**, and **32** were compared side-by-side (Figure 4), it was observed that ethanolaminopropyl and aminopropyl derivatives **31** and **32** behave similarly to **19**. One possible reason for the decrease in

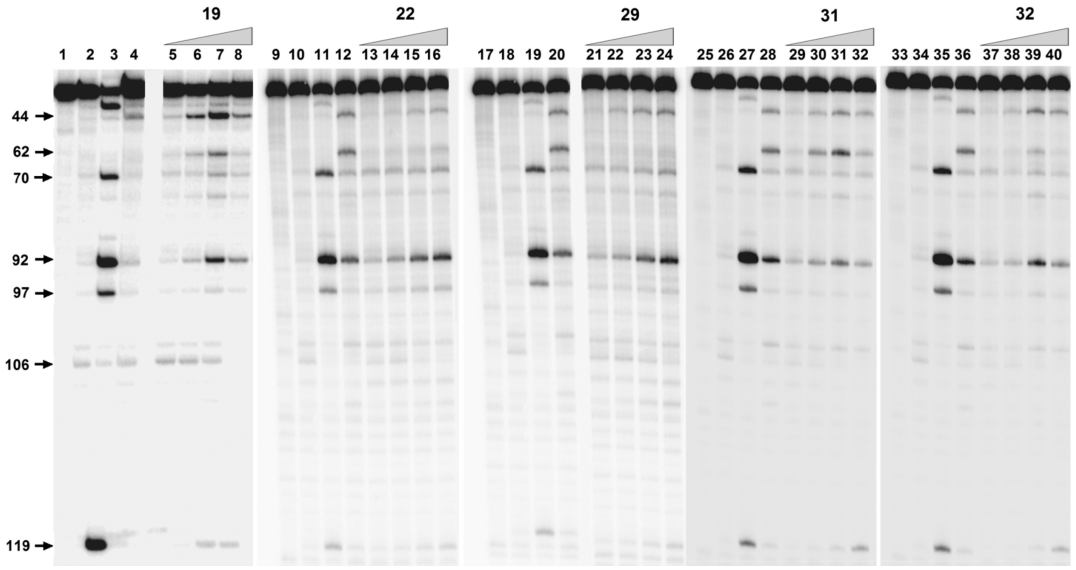

Figure 4. Lanes 1, 9, 17, 25, 33: DNA alone. Lanes 2, 10, 18, 26, 34: Top1 alone. Lanes 3, 11, 19, 27, 35: Top1 + **1** (1 μM). Lane 4: Top1 + **2** (100 μM). Lanes 12, 20, 28, 36: Top1 + **3a** (1 μM). Lanes 5−8: Top1 + **19** at 0.1, 1, 10, 100 μM. Lanes 13−16: Top1 + **22** at 0.1, 1, 10, 100 μM. Lanes 21−24: Top1 + **29** at 0.1, 1, 10, 100 μM. Lanes 29−32: Top1 + **31** at 0.1, 1, 10, 100 μM. Lanes 37−40: Top1 + **32** at 0.1, 1, 10, 100 μM. Numbers on right and arrows show the cleavage site positions.

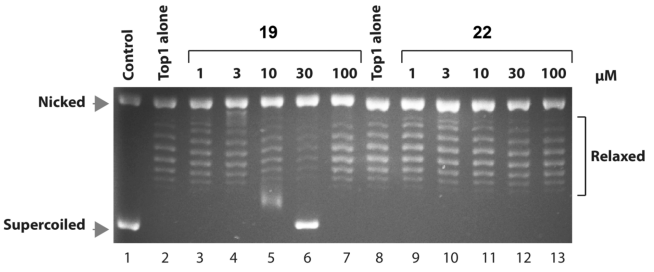

Figure 5. DNA unwinding and Top1 inhibition by **19** and **22**. Lane 1: DNA alone. Lanes 2 and 8 were DNA + Top1. Lanes 3−7: DNA + Top1 + **19** at 1, 3, 10, 30, 100 μM. Lanes 9−13: DNA + Top1 + **22** at 1, 3, 10, 30, 100 μM.

DNA cleavage at high drug concentration is that intercalation of these indenoisoquinolines into DNA makes it a poorer enzyme substrate. In contrast, the morpholinopropyl and imidazolylpropyl analogues **22** and **29** express concentration-dependent increase of intensity of DNA cleavage bands, and therefore, Top1 inhibitory activity, up to 100 μM.

DNA unwinding assays have been performed in order to test the DNA intercalation hypothesis for the observed decrease in DNA cleavage at high drug concentration. Two compounds have been tested and compared in this assay: dimethylaminopropyl analogue **19** and morpholinopropyl compound **22** (Figure 5). DNA unwinding reactions were performed in two steps as described.[31] First, SV40 DNA was reacted with excess of Top1 for 15 min at 37 °C in the absence of drug to fully relax the DNA. The relaxed DNA was then further incubated for 30 min at 37 °C in the presence of increasing concentrations of drugs (Figure 5). Additional incubation of the DNA and Top1 for 30 min at 37 °C in the absence of drug was performed as a control. The results of the DNA unwinding assay demonstrated the ability of **19** to unwind DNA at concentrations above 3 μM in a concentration-dependent manner, hence showing the ability of **19** to intercalate into free DNA. At its highest tested concentration, 100 μM, compound **19** completely inhibits the Top1-mediated DNA relaxation, as demonstrated by the fact that there is no more detectable relaxation by Top1 after addition of the drug. The results of the experiment with compound **22**, on the other hand, show its inability to unwind/intercalate into DNA in the range of tested concentrations, 1−100 μM. These results can presumably be extrapolated to other aminopropyl derivatives presented in this work.

This observation might also explain the lack of correlation between Top1 inhibitory activity and cytotoxicity in the series of compounds. The ability to intercalate into free DNA can potentially serve as an off-target effect of the drug, increasing its cytotoxicity. On the other hand, the Top1 inhibitory activity as observed in Top1-mediated DNA cleavage assays can decrease as the ability to intercalate into free DNA increases.

Most azaindenoisoquinolines retained the activity of the "classical" indenoisoquinolines. Introduction of the pyridine nitrogen (a strong hydrogen bond acceptor) into the core of the indenoisoquinoline structure should also improve aqueous solubility. To test this hypothesis, the solubilities of two 7-azaindenoisoquinolines were assessed and compared to that of closely related "classical" indenoisoquinolines (Figure 6). Aqueous solubility was determined by an HPLC method.[32] For this test, the samples of four different indenoisoquinolines (Figure 6) were shaken with 1 M Tris buffer (pH 7.5) solution. The aliquots of the supernatants were injected into the HPLC system after 24 h. In order to determine the concentration of the sample, one point calibration was done against standards with known concentrations of the sample compounds. The estimation of the solubility demonstrated that the introduction of a pyridine ring into the indenoisoquinoline system led to a significant increase of the water solubility. Interestingly, the increase in solubility of the drug did not compromise the Top1 inhibitory activity or cytotoxicity of the drugs (Figure 6, Table 1). A similar result was observed when an extra nitrogen was introduced into the

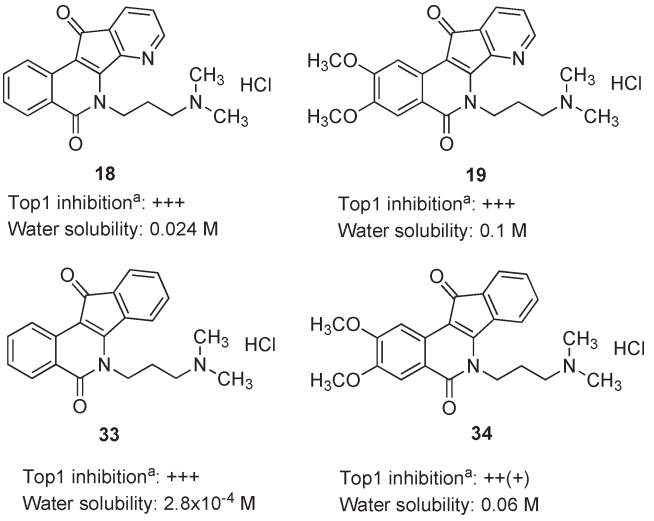

Figure 6. Solubility of indenoisoquinolines.

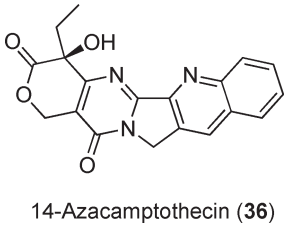

Figure 7. Structure of 14-azacamptothecin.

polycyclic system of **1**, resulting in 14-azacamptothecin (**36**, Figure 7), which possessed greater water solubility compared to the parent **1**.[33,34]

Crystallography of the ternary complexes of indenoisoquinolines revealed that only one major polar interaction between drug and the Top1-DNAcc is present, which is a hydrogen bond to the Arg364.[7] It was therefore hypothesized that $\pi-\pi$ stacking interactions play a major role in complex stabilization and that these interactions determine the orientations of the drugs within ternary complexes. This hypothesis was supported by a series of high level ab initio calculations on a number of diverse Top1 inhibitors.[35−37] Thus, drug binding orientations and DNA site specificities were calculated correctly for a number of different ligands.[35−37]

To investigate the effect of the introduction of nitrogen into the aromatic systems of indenoisoquinolines on their abilities to form strong $\pi-\pi$ stacking interactions, a series of hypothetical indenoisoquinoline structures were modeled and subjected to MP2 single point energy calculations. In order to derive a model for such calculations, an inhibitor and adjacent base pairs were taken from the X-ray structure of **4**−Top1−DNA ternary complex (PDB entry 1SC7).[7] The deoxyribose rings of the DNA bases and the carboxypropyl chain of **4** were replaced with methyl groups, similar to the previously described model.[37] The geometry optimizations and frequency calculation at the HF/6-31G** level were performed on the indenoisoquinoline molecule, as well as A−T and G−C base pairs using the Gaussian 09[38] software package. The original complex was then replaced with the geometry-optimized parts (Figure 8). The MP2 single point energy calculation with the 6-31G* basis set was done with the resulting complex.

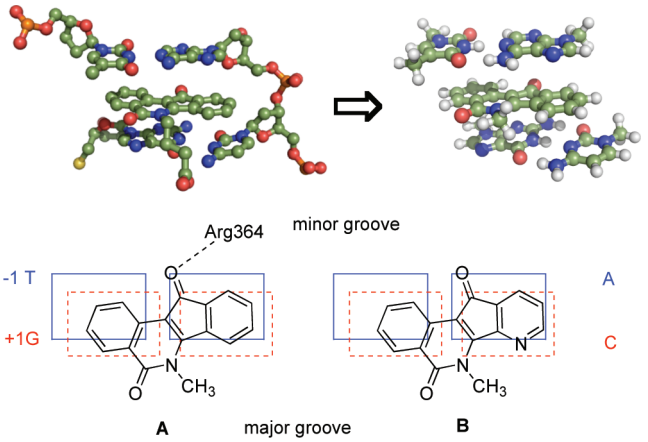

Figure 8. Derivation of indenoisoquinoline−DNA "sandwich" complex models for quantum mechanical calculations.

Table 2. $\pi-\pi$ Staking Interaction Energies of Models A and B

model	$E_{int,vac}$ (kcal/mol)[a]	$E_{int,aq}$ (kcal/mol)[a]	E_{corr} (kcal/mol)[b]	charge transfer (e^-)[c]
A	−6.95	−15.17	−26.0284	0.0115
B	−7.99	−15.57	−25.7899	0.0126

[a] E_{int} is derived from MP2/6-31G* single point energy calculations. [b] $E_{corr} = E_{int(MP2/6\text{-}31G^*)} - E_{int(HF/6\text{-}31G^*)}$. [c] The magnitude of the charge transfer as estimated by NBO analysis at HF/6-31G** level.

The CH group in position 7 of the D-ring of the inhibitor was replaced with nitrogen to produce the 7-azaindenoisoquinoline model (Figure 8). Before fitting of azaindenoisoquinolines into their corresponding complexes with DNA base pairs, geometry optimizations were performed. After the complexes were assembled, MP2/6-31G* single point energy calculations were performed. The basis set superposition error (BSSE) for each complex was calculated, specifying two fragments: the first was two flanking DNA base pairs, and the second was the intercalating indenoisoquinoline inhibitor. The in vacuo $\pi-\pi$ stacking interaction energy was then calculated as $E_{int,vac} = E_{complex,vac} - E_{ligand,vac} - E_{bp,vac}$ + BSSE, where $E_{complex,vac}$, $E_{ligand,vac}$, and $E_{bp,vac}$ are the corresponding MP2/6-31G* calculated energies of complex, ligand, and DNA base pairs at their normal distance in the absence of intercalator (Table 2). Similarly, the energy of the $\pi-\pi$ staking interaction was also calculated in water ($E_{int,aq}$) using the polarized continuum model. The dispersion and charge transfer interaction components of the $\pi-\pi$ staking have also been determined. The dispersion (electron correlation) interaction (E_{corr}) was defined as the difference of energy calculated by MP2 and HF methods at the 6-31G* level, $E_{corr} = E_{int(MP2)} - E_{int(HF)}$ (Table 2). Natural bond orbital (NBO)[39] analyses have been performed at the HF/6-31G** level of theory to determine the charge transfer component (Table 2). The results of these calculations showed that the slight decrease in the dispersion force was outweighed by the increased charge transfer, leading to an overall greater $\pi-\pi$ stacking interaction energy for the 7-azaindenoiusoquinoline (model **B**, Figure 8) vs the indenoisoquinoline (model **A**, Figure 8) both in vacuo ($E_{int,vac}$) and in water ($E_{int,aq}$).

In conclusion, a series of novel azaindenoisoquinolines have been prepared. Two alternative derivatization pathways have

been explored, and the established protocols were then used to synthesize diverse products. All synthesized compounds were evaluated in Top1-mediated DNA cleavage reactions in order to establish the extent of their abilities to stabilize Top1-DNAcc and hence their Top1 inhibitory activities. The NCI screening for antiproliferative activity demonstrated a slight but consistent improvement of the cytotoxic properties of the azaindenoisoquinoline series over identically substituted, previously described indenoisoquinolines. The role of the aminopropyl chain was also investigated and demonstrated to play a crucial role in biological activity, consistent with prior results for indenoisoquinolines. The results of the DNA unwinding assay presented in this work unambiguously show the effect this group has on the ability of the drug to intercalate into both free DNA and Top1-DNAcc. Smaller amines (e.g., **17**) allow intercalation into DNA in the absence of Top1, while larger ones (e.g., **20**) do not. This explains why indenoisoquinolines with smaller amines suppress DNA cleavage by Top1 at high drug concentrations.

EXPERIMENTAL SECTION

General. Melting points were determined using capillary tubes with a Mel-Temp apparatus and are uncorrected. The nuclear magnetic resonance spectra (^{1}H and ^{13}C NMR) were recorded using ARX300 300 MHz and DRX500 500 MHz Bruker NMR spectrometers. IR spectra were recorded using a Perkin-Elmer 1600 series FTIR spectrometer. Purity of all tested compounds was ≥95%, as established by combustion analysis. Combustion microanalyses were performed at the Purdue University Microanalysis Laboratory or Galbraith Laboratories Inc., and the reported values were within 0.4% of the calculated values. HPLC analyses were performed on a Waters 1525 binary HPLC pump/Waters 2487 dual λ absorbance detector system. Analytical thin-layer chromatography was carried out on Baker-flex silica gel IB2-F plates, and compounds were visualized with short wavelength UV light. Silica gel flash chromatography was performed using 230−400 mesh silica gel.

General Procedure for the Preparation of 7-Aza-5,6-dihydro-5-oxo-11*H*-indeno[1,2-*c*]isoquinolines 12−14. 3-Methylpicolonitrile (**10**, 3.0−4.0 g, 25.4−33.9 mmol, 1 equiv), NBS (6.78−9.04 g, 38.1−50.8 mmol, 1.5 equiv), and AIBN (0.42−0.56 g, 2.5−3.4 mmol, 0.1 equiv) were diluted with 1,2-dichloroethane (80−100 mL), and the reaction mixture was heated at reflux for 2 h. The reaction mixture was concentrated to half its original volume, filtered, and the filtrate was concentrated to dryness to provide crude **11**. Compound **11** was diluted with acetonitrile (100−125 mL). The appropriate homophthalic anhydride (**5**, **6**, or **7**, 6.8−12.4 g, 41.9−55.9 mmol, 1.65 equiv) was added, followed by triethylamine (18−24 mL, 127.0−169.5 mmol, 5 equiv), and the solution was heated at reflux for 10 h. The solution was allowed to cool to room temperature and the precipitate was filtered and washed with hot acetonitrile (2 × 35 mL) to provide the desired compound.

General Procedure for the Preparation of 7-Aza-5,6-dihydro-5,11-dioxo-11*H*-indeno[1,2-*c*]isoquinolines 15−17. The appropriate 7-aza-5,6-dihydro-5-oxo-11*H*-indeno[1,2-*c*]isoquinoline (**12**−**14**, 0.50−1.0 g, 1.8−4.27 mmol, 1 equiv) and SeO_2 (0.4−0.95 g, 3.6−8.54 mmol, 2 equiv) were diluted with 1,4-dioxane (125−250 mL) and heated at reflux for 16 h. The reaction mixture was filtered, the filtrate was concentrated, and the precipitate was washed with MeOH (2 × 50 mL) to provide the desired product.

General Procedure for the Preparation of 7-Azaindenoisoquinolines 18−23. The appropriate 7-aza-5,6-dihydro-5,11-dioxo-11*H*-indeno[1,2-*c*]isoquinoline (**15**−**17**, 94−248 mg, 0.31−1.0 mmol, 1 equiv) and triphenylphosphine (262−786 mg, 1.0−3.0 mmol, 3 equiv) were diluted in THF (16−50 mL). The appropriate alcohol [3-dimethylamino-1-propanol (0.17−0.21 mL, 1.46−1.82 mmol, 3 equiv) or 3-morpholinopropan-1-ol (145−435 mg, 1.0−3.0 mmol, 3 equiv)] was added, followed by DIAD (202−606 mg, 1.0−3.0 mmol, 3 equiv). The solution was stirred at room temperature for 64 h. As the reaction reached completion, all of the solid material dissolved. The reaction mixture was concentrated to dryness. The solid was purified by flash column chromatography (SiO_2), eluting with 1% MeOH in $CHCl_3$, to provide a dark-orange solid. The solid was further purified by treating it with 3 M HCl in methanol (15 mL) for 2 h at room temperature with stirring. The solution was concentrated to dryness. The orange solid was diluted in ethyl ether (50 mL). The hydrochloride salt of the product precipitated and was collected using vacuum filtration, washing with ethyl ether (3 × 15 mL), to provide an orange solid.

General Procedure for the Preparation of 7-Azaindenoisoquinolines 21−25 and 29−31. Sodium hydride (95%, 50 mg, 2 mmol, 2 equiv) was added to a mixture of the appropriate 7-aza-5,6-dihydro-5,11-dioxo-11*H*-indeno[1,2-*c*]isoquinoline (**15**, 243 mg, 1 mmol, 1 equiv, or **16**, 308 mg, 1 mmol, 1 equiv) and DMF (6 mL) at −5 °C, and the resulting mixture was allowed to warm to room temperature over 3 h. The resulting clear dark red solution was cooled to −5 °C, and 1,3-dibromopropane (788 mg, 4 mmol, 4 equiv) was added. The solution was stirred at room temperature for 12 h. The reaction mixture was quenched with water (50 mL). The products were extracted with chloroform (3 × 10 mL). The combined extracts were washed with water (3 × 10 mL), brine (10 mL), dried with sodium sulfate, and concentrated under reduced pressure. The residue was subjected to flash column chromatography (silica gel, $CHCl_3$). The appropriate amine (140.3−200 mg, 2.3 mmol, 2.3 equiv) was added to a solution of crude intermediate in 1,4-dioxane (10 mL). The resulting mixture was heated to reflux for 6 h. The solvent was evaporated under reduced pressure, and the residue was redissolved in chloroform (30 mL). The chloroform solution was washed with water (3 × 5 mL), brine (5 mL), dried with sodium sulfate, and evaporated to dryness. The solid residue was subjected to flash column chromatography (silica gel), eluting with chloroform, to get **24** and **25**, and then with 5−15% methanol in chloroform to obtain **21**−**23** and **29**−**31**.

7-Aza-5,6-dihydro-5-oxo-11*H*-indeno[1,2-*c*]isoquinoline (12). The general procedure provided the desired compound as a gray solid (2.49 g, 31%): mp 267−269 °C. IR (KBr) 3098, 1665, 1573, 1478, 767, and 756 cm^{-1}; ^{1}H NMR (DMSO-d_6) δ 12.18 (s, 1 H), 8.56 (dd, J = 4.9 and 1.3 Hz, 1 H), 8.30 (d, J = 8.0 Hz, 1 H), 8.02 (dd, J = 7.5 and 1.1 Hz, 1 H), 7.82−7.80 (m, 2 H), 7.57−7.51 (m, 1 H), 7.36 (dd, J = 7.5 and 5.0 Hz, 1 H), 3.94 (s, 2 H); ESIMS m/z (rel intensity) 235 (MH^+, 100). Anal. Calcd for $C_{15}H_{10}N_2O$: C, 76.91; H, 4.30; N, 11.96. Found: C, 76.58; H, 4.16; N, 11.80.

7-Aza-5,6-dihydro-2,3-dimethoxy-5-oxo-11*H*-indeno[1,2-*c*]isoquinoline (13). The general procedure provided the desired compound as a purple solid (3.87 g, 39%): mp 284−286 °C. IR (KBr) 3399, 3276, 1635, 1604, 1479, 1215, and 803 cm^{-1}; ^{1}H NMR (DMSO-d_6) δ 11.99 (s, 1 H), 8.52 (dd, J = 4.9 and 1.1 Hz, 1 H), 7.95 (d, J = 6.9 Hz, 1 H), 7.67 (s, 1 H), 7.32 (dd, J = 7.5 and J = 4.9, 1 H), 7.24 (s, 1 H), 3.97 (s, 3 H), 3.91 (s, 2 H), 3.89 (s, 3 H); ESIMS m/z (rel intensity) 295 (MH^+, 100).

7-Aza-5,6-dihydro-3-nitro-5-oxo-11*H*-indeno[1,2-*c*]isoquinoline (14). The general procedure provided the desired compound as a green solid (878 mg, 12%): mp 323 °C. IR (KBr) 3096, 1691, 1607, 1508, 1330, and 834 cm^{-1}; ^{1}H NMR (DMSO-d_6, 500 MHz) δ 12.74 (s, 1 H), 8.95 (d, J = 2.3 Hz, 1 H), 8.60 (d, J = 4.9 Hz, 1 H), 8.52 (d, J = 2.3 Hz, 1 H), 8.51 (d, J = 2.6 Hz, 1 H), 8.06 (d, J = 8.0 Hz, 1 H), 8.00 (d, J = 8.0 Hz, 1 H), 7.41 (dd, J = 7.6 and 4.9 Hz, 1 H), 3.97 (s, 3 H), 3.91 (s, 2 H), 3.89 (s, 3 H); negative ion ESIMS m/z (rel intensity) 278 [$(M - H^+)^-$, 100].

7-Aza-5,6-dihydro-5,11-dioxo-11*H*-indeno[1,2-*c*]isoquinoline (15). The general procedure provided the desired compound as a red-orange solid (0.94 g, 89%): mp 337 °C (dec). IR (KBr) 2979, 1678,

1575, 1085, and 770 cm^{-1}; ^1H NMR (DMSO-d_6) δ 13.12 (s, 1 H), 8.61 (dd, J = 6.2 and 1.4 Hz, 1 H), 8.44 (d, J = 7.9 Hz, 1 H), 8.23 (d, J = 7.3 Hz, 1 H), 7.89−7.81 (m, 2 H), 7.58−7.53 (m, 1 H), 7.46 (dd, J = 7.3 and 5.2 Hz, 1 H); negative ion ESIMS m/z (rel intensity) 247 [$(M - H^+)^-$, 100].

7-Aza-5,6-dihydro-2,3-dimethoxy-5,11-dioxo-11*H*-indeno-[1,2-*c*]isoquinoline (16). The general procedure provided the desired compound as a dark red solid (272 mg, 26%): mp 358−359 °C. IR (KBr) 3129, 2988, 1676, 1504, 1277, and 777 cm^{-1}; ^1H NMR (DMSO-d_6) δ 12.96 (s, 1 H), 8.56 (dd, J = 6.2 and 1.4 Hz, 1 H), 7.86−7.81 (m, 2 H), 7.59 (s, 1 H), 7.40 (t, J = 6.8 Hz, 1 H); negative ion ESIMS m/z (rel intensity) 307 [$(M - H^+)^-$, 100].

7-Aza-5,6-dihydro-3-nitro-5,11-dioxo-11*H*-indeno[1,2-*c*]isoquinoline (17). The general procedure provided the desired compound as a red-orange solid (310 mg, 59%): mp 351−353 °C. IR (KBr) 3187, 1692, 1567, 1335, and 785 cm^{-1}; ^1H NMR (DMSO-d_6) δ 13.75 (s, 1 H), 8.86 (s, 1 H), 8.69 (dd, J = 5.2 and 1.3 Hz, 1 H), 8.55 (s, 2 H), 7.97 (dd, J = 7.4 and 1.3 Hz, 1 H), 7.53 (dd, J = 7.4 and 5.2 Hz 1 H); negative ion ESIMS m/z (rel intensity) 292 [$(M - H^+)^-$, 100].

7-Aza-5,6-dihydro-6-(3-dimethylaminopropyl)-5,11-dioxo-11*H*-indeno[1,2-*c*]isoquinoline Hydrochloride (18). The general procedure provided the desired compound as an orange solid (160 mg, 59%): mp 268−270 °C. IR (KBr) 3446, 1703, 1670, 1505, and 770 cm^{-1}; ^1H NMR (DMSO-d_6) δ 10.05 (s, 1 H), 8.66 (dd, J = 1.5 and 5.2 Hz, 1 H), 8.56 (d, J = 7.8 Hz, 1 H), 8.27 (d, J = 7.5 Hz, 1 H), 7.95 (dd, J = 1.5 Hz and 7.4, Hz 1 H), 7.90−7.84 (m, 1 H), 7.63−7.58 (m, 1 H), 7.50 (dd, J = 5.2 and 7.3 Hz, 1 H), 4.92 (t, J = 6.8 Hz, 2 H), 3.23 (p, J = 5.3 and 10.1 Hz, 2 H), 2.75 (s, 3 H), 2.74 (s, 3 H), 2.22−2.17 (m, 2 H); positive ion ESIMS m/z (rel intensity) 333 [(MH^+), 100]. Anal. Calcd for $C_{20}H_{19}N_3O_2 \cdot HCl \cdot 1.5H_2O$: C, 60.53; H, 5.84; N, 10.59. Found: C, 60.36; H, 5.62; N, 10.45.

7-Aza-5,6-dihydro-6-(3-dimethylaminopropyl)-2,3-dimethoxy-5,11-dioxo-11*H*-indeno[1,2-*c*]isoquinoline Hydrochloride (19). The general procedure provided the desired compound as a light-orange solid (158 mg, 76%): mp 278−281 °C (dec). IR (KBr) 3407, 2456, 1702, 1654, 1476, and 779 cm^{-1}; ^1H NMR (DMSO-d_6) δ 9.99 (s, 1 H), 8.59 (dd, J = 1.2 and 5.2 Hz, 1 H), 7.88 (s, 1 H), 7.85 (d, J = 7.3 Hz, 1 H), 7.54 (s, 1 H), 7.43 (dd, J = 5.3 and 7.3 Hz, 1 H), 4.86 (t, J = 6.4 Hz, 1 H), 3.93 (s, 3 H), 3.88 (s, 3 H), 3.21−3.16 (m, 3 H), 2.76 (s, 3 H), 2.74 (s, 3 H), 2.19−2.15 (m, 2 H); positive ion ESIMS m/z (rel intensity) 394 [(MH^+), 100]. Anal. Calcd for $C_{22}H_{23}N_3O_4 \cdot 2HCl \cdot 0.5H_2O$: C, 55.47; H, 5.45; N, 10.59. Found: C, 55.59; H, 5.51; N, 8.84.

7-Aza-5,6-dihydro-6-(3-dimethylaminopropyl)-3-nitro-5,11-dioxo-11*H*-indeno[1,2-*c*]isoquinoline Hydrochloride (20). The general procedure provided the desired compound as a bright orange solid (130 mg, 62%): mp 280−282 °C (dec). IR (KBr) 3393, 1705, 1677, 1501, 1338, and 791 cm^{-1}; ^1H NMR (DMSO-d_6) δ 9.88 (s, 1 H), 8.94 (d, J = 2.3 Hz, 1 H), 8.74 (dd, J = 3.9 and 4.4 Hz, 2 H), 8.67 (dd, J = 2.5 and 8.9 Hz, 1 H), 8.08 (dd, J = 1.7 and 6.6 Hz, 1 H), 7.60 (dd, J = 5.2 and 7.4 Hz, 1 H), 4.97 (t, J = 6.6, 2 H), 3.26−3.21 (m, 2 H), 2.77 (s, 3 H), 2.75 (s, 3 H), 2.25 (m, 2 H); positive ion ESIMS m/z (rel intensity) 379 (MH^+, 100). Anal. Calcd for $C_{20}H_{18}N_4O_4 \cdot HCl \cdot 1.5H_2O$: C, 54.36; H, 5.02; N, 12.68. Found: C, 54.13; H, 4.69; N, 12.52.

7-Aza-5,6-dihydro-6-(3-morpholinopropyl)-5,11-dioxo-11*H*-indeno[1,2-*c*]isoquinoline Hydrochloride (21). The general procedure provided the desired compound as an orange solid (255 mg, 62%): mp 316−318 °C. IR (KBr) 1704, 1669, 1612, 1570, 1550, 1506, 779 cm^{-1}; ^1H NMR (DMSO-d_6) δ 10.40 (s, 1 H), 8.61 (d, J = 4.5 Hz, 1 H), 8.54 (d, J = 7.8 Hz, 1 H), 7.92 (dd, J = 7.2, 1.5 Hz, 1 H), 7.86 (t, J = 7.2 Hz, 1 H), 7.56 (t, J = 7.2 Hz, 1 H), 7.45 (dd, J = 7.5 and 6.6 Hz, 1 H), 4.91 (m, 2 H), 3.90 (m, 2 H), 3.69 (m, 2 H), 3.37 (m, 2 H), 3.05 (m, 4 H), 2.24 (m, 2 H). Anal. Calcd for $C_{22}H_{21}N_3O_3 \cdot HCl \cdot 1.5H_2O$: C, 60.20; H, 5.74; N, 9.57. Found: C, 60.37; H, 5.83; N, 9.62.

7-Aza-5,6-dihydro-6-(3-morpholinopropyl)-2,3-dimethoxy-5,11-dioxo-11*H*-indeno[1,2-*c*]isoquinoline Hydrochloride (22). The general procedure provided the desired compound as a red solid (109 mg, 68%): mp 322−324 °C. IR (KBr) 1735, 1704, 1655, 1642, 1607, 1552, 1513 cm^{-1}; ^1H NMR ($CDCl_3$) δ 8.37 (dd, J = 5.4 and 1.5 Hz, 1 H), 7.86 (s, 1 H), 7.61 (dd, J = 7.2 and 1.5 Hz, 1 H), 7.54 (s, 1 H), 7.11 (dd, J = 7.2 and 5.1 Hz, 1 H), 4.91 (m, 2 H), 3.97 (s, 3 H), 3.91 (s, 3 H), 3.43 (m, 4 H), 2.44 (m, 2 H), 2.34 (m, 4 H), 1.95 (m, 2 H); positive ion ESIMS m/z (rel intensity) 436 [(MH^+), 100]. Anal. Calcd for $C_{24}H_{25}N_3O_5 \cdot HCl \cdot 2.5H_2O$: C, 55.76; H, 6.04; N, 8.13. Found: C, 55.83; H, 5.87; N, 8.33.

7-Aza-5,6-dihydro-6-(3-morpholinopropyl)-3-nitro-5,11-dioxo-11*H*-indeno[1,2-*c*]isoquinoline Hydrochloride (23). The general procedure provided the desired compound as a light-red solid (69 mg, 30%): mp 266−228 °C. IR (KBr) 1705, 1679, 1614, 1598, 1556, 1502 cm^{-1}; ^1H NMR (DMSO-d_6) δ 10.28 (s, 1 H), 8.96 (d, J = 2.4 Hz, 1 H), 8.78−8.75 (m, 2 H), 8.67 (dd, J = 9.0 and 2.4 Hz, 1 H), 8.08 (d, J = 7.2 Hz, 1 H), 7.60 (dd, J = 7.2 and 5.1 Hz, 1 H), 4.98 (m, 2 H), 3.98 (m, 2 H), 3.40 (m, 2 H), 3.09 (m, 4 H), 2.29 (m, 2 H). Anal. Calcd for $C_{22}H_{20}N_4O_5 \cdot 0.8H_2O$: C, 60.77; H, 5.01; N, 12.88. Found: C, 60.92; H, 4.71; N, 12.56.

7-Aza-5,6-dihydro-6-allyl-5,11-dioxo-11*H*-indeno[1,2-*c*]isoquinoline (24). The general procedure provided the desired compound as a red solid (37−150 mg, 13−52%): mp 222−224 °C. IR (KBr) 1700, 1666, 1644, 1611, 1568, 1548, 1501 cm^{-1}; ^1H NMR ($CDCl_3$) δ 8.66 (d, J = 7.8 Hz, 1 H), 8.52 (dd, J = 5.1 and 1.5 Hz, 1 H), 8.38 (d, J = 7.5 Hz, 1 H), 7.81−7.73 (m, 2 H), 7.52 (t, J = 8.1 Hz, 1 H), 7.24 (dd, J = 7.5 and 5.4 Hz, 1 H), 6.11 (m, 1 H), 5.67 (d, J = 5.7 Hz, 1 H), 5.32−5.19 (m, 2 H). Anal. Calcd for $C_{18}H_{12}N_2O_2 \cdot 0.2H_2O$: C, 74.06; H, 4.28; N, 9.60. Found: C, 73.97; H, 4.14; N, 9.53.

7-Aza-5,6-dihydro-6-allyl-2,3-dimethoxy-5,11-dioxo-11*H*-indeno[1,2-*c*]isoquinoline (25). The general procedure provided the desired compound as a dark-red solid (73−122 mg, 21−35%): mp 266−268 °C. IR (KBr) 1701, 1659, 1608, 1570, 1552, 1515 cm^{-1}; ^1H NMR ($CDCl_3$) δ 8.47 (dd, J = 5.4, 1.5 Hz, 1 H), 8.03 (s, 1 H), 7.74−7.71 (m, 2 H), 7.18 (dd, J = 7.5, 5.4 Hz, 1 H), 6.01 (m, 1 H), 5.62 (d, J = 5.7 Hz, 2 H), 5.3−5.17 (m, 2 H), 4.06 (s, 3 H), 3.99 (s, 3 H). Anal. Calcd for $C_{20}H_{16}N_2O_4 \cdot 0.2H_2O$: C, 68.25; H, 4.70; N, 7.96. Found: C, 61.21; H, 4.63; N, 7.90.

7-Aza-5,6-dihydro-6-(3-(1*H*-imidazol-1-yl)propyl)-5,11-dioxo-11*H*-indeno[1,2-*c*]isoquinoline (28). The general procedure provided the desired compound as an orange solid (59 mg, 17%): mp 200−202 °C. IR (KBr) 1698, 1664, 1610, 1570, 1549, 1506 cm^{-1}; ^1H NMR ($CDCl_3$) δ 8.64 (d, J = 8.1 Hz, 1 H), 8.43 (dd, J = 5.1, 1.5 Hz, 1 H), 8.37 (d, J = 7.2 Hz, 1 H), 7.80−7.72 (m, 2 H), 7.58 (s, 1 H), 7.53 (m, 2 H), 7.23 (dd, J = 7.5, 5.4 Hz, 1 H), 7.09 (s, 1 H), 7.01 (s, 1 H), 5.00 (t, J = 7.5 Hz, 2 H), 4.17 (t, J = 6.9 Hz, 2 H), 2.36 (quint, J = 7.5 Hz, 2 H); positive ESIMS m/z (rel intensity) 357 (MH^+, 100). Anal. Calcd for $C_{21}H_{16}N_4O_2 \cdot 0.6H_2O$: C, 68.69; H, 4.72; N, 15.26. Found: C, 68.98; H, 4.62; N, 14.82.

7-Aza-5,6-dihydro-6-(3-(1*H*-imidazol-1-yl)propyl)-2,3-dimethoxy-5,11-dioxo-11*H*-indeno[1,2-*c*]isoquinoline (29). The general procedure provided the desired compound as a purple solid (69 mg, 17%): mp 238−240 °C. IR (KBr) 1699, 1649, 1609, 1570, 1552, 1516 cm^{-1}; ^1H NMR ($CDCl_3$) δ 8.38 (dd, J = 5.1, 1.5 Hz, 1 H), 8.0 (s, 1 H), 7.72 (dd, J = 7.5, 1.8 Hz, 1 H), 7.67 (s, 1 H), 7.56 (s, 1 H), 7.19 (dd, J = 7.5, 5.4 Hz, 1 H), 7.07 (s, 1 H), 6.99 (s, 1 H), 4.96 (t, J = 7.5 Hz, 2 H), 4.15 (t, J = 7.2 Hz, 2 H), 4.04 (s, 3 H), 3.99 (s, 3 H), 2.33 (quint, J = 7.2 Hz, 2 H); positive ESIMS m/z (rel intensity) 349 (100), 417 (MH^+, 61). Anal. Calcd for $C_{23}H_{20}N_4O_4 \cdot 0.5H_2O$: C, 64.93; H, 4.98; N, 13.17. Found: C, 65.13; H, 4.88; N, 12.70.

7-Aza-5,6-dihydro-6-(3-(2-hydroxyethylamino)propyl)-5,11-dioxo-11*H*-indeno[1,2-*c*]isoquinoline Hydrochloride (30). The general procedure provided the desired compound. The product was redissolved in chloroform (5 mL), and HCl solution in methanol

(3 M, 1 mL) was added. The resulting solution was evaporated to dryness to obtain an orange solid (58 mg, 16%): mp 258−262 °C (dec). IR (KBr) 1711, 1665, 1611, 1569, 1549, 1503 cm^{-1}; ^1H NMR ($CDCl_3$) δ 8.73 (s, 2 H), 8.64 (dd, J = 5.1, 1.5 Hz, 1 H), 8.51 (d, J = 7.8 Hz, 1 H), 8.24 (d, J = 8.1 Hz, 1 H), 7.91 (dd, J = 7.5, 1.5 Hz, 1 H), 7.86 (t, J = 7.5 Hz, 1 H), 7.59 (t, J = 8.1 Hz, 1 H), 7.46 (dd, J = 7.2, 5.1 Hz, 1 H), 4.89 (t, J = 6.6 Hz, 2 H), 3.63 (t, J = 5.1 Hz, 2 H), 3.05−2.98 (m, 4 H), 2.19 (m, 2 H); positive ESIMS m/z (rel intensity) 350 (MH^+ 100), 289 (74). Anal. Calcd for $C_{20}H_{19}N_3O_3 \cdot HCl \cdot H_2O$: C, 59.22; H, 5.52; N, 10.36. Found: C, 58.98; H, 5.02; N, 10.10.

7-Aza-5,6-dihydro-6-(3-(2-hydroxyethylamino)propyl)-2,3-dimethoxy-5,11-dioxo-11*H*-indeno[1,2-*c*]isoquinoline Hydrochloride (31). The general procedure provided the desired compound. The product was redissolved in chloroform (5 mL), and HCl solution in methanol (3 M, 1 mL) was added. The resulting solution was evaporated to dryness to obtain a purple solid (83 mg, 20%): mp 280−282 °C (dec). IR (KBr) 1703, 1639, 1609, 1594, 1570, 1553, 1516 cm^{-1}; ^1H NMR (DMSO-d_6) δ 8.72 (s, 2 H) 8.57 (d, J = 5.1 Hz, 1 H), 7.83 (s, 1 H), 7.81 (d, J = 7.5 Hz, 1 H), 7.49 (s, 1 H), 7.56 (s, 1 H), 7.39 (dd, J = 7.2, 5.4 Hz, 1 H), 5.25 (s, 1 H), 4.82 (t, J = 6.3 Hz, 2 H),, 3.90 (s, 3 H), 3.86 (s, 3 H), 3.63 (s, 2 H), 2.98 (s, 4 H), 2.16 (m, 2 H); positive ESIMS m/z (rel intensity) 410 (MH^+, 100). Anal. Calcd for $C_{22}H_{23}N_3O_5 \cdot HCl \cdot H_2O$: C, 56.96; H, 5.65; N, 9.06. Found: C, 56.65; H, 5.24; N, 9.08.

7-Aza-5,6-dihydro-6-(3-aminopropyl)-2,3-dimethoxy-5,11-dioxo-11*H*-indeno[1,2-*c*]isoquinoline Hydrochloride (32). Sodium hydride (95%, 50 mg, 2 mmol) was added to a mixture of 7-aza-5,6-dihydro-2,3-dimethoxy-5,11-dioxo-11*H*-indeno[1,2-*c*]isoquinoline (**16**, 308 mg, 1 mmol) and DMF (6 mL) at −5 °C, and the resulting mixture was allowed to warm to room temperature over 3 h. The resulting clear dark red solution was cooled to −5 °C, and 1,3-dibromopropane (788 mg, 4 mmol) was added. The solution was stirred at room temperature for 12 h. The reaction mixture was quenched with water (50 mL). The products were extracted with chloroform (3 × 10 mL). The combined extracts were washed with water (3 × 10 mL), brine (10 mL), dried with sodium sulfate, and concentrated under reduced pressure. The residue was subjected to flash column chromatography (silica gel, $CHCl_3$) to provide a mixture of **25** and **27** that was further used without additional purification or separation. Sodium azide (650 mg, 10 mmol) was added to a solution of the mixture of **25** and **27** in DMF (5 mL). The resulting mixture was stirred at room temperature for 12 h. Water (50 mL) was added to the mixture, and the products were extracted with chloroform (3 × 10 mL). The chloroform solution was washed with water (3 × 10 mL), brine (10 mL), dried with sodium sulfate, and evaporated to dryness. The residue was redissolved in benzene (10 mL), and triethyl phosphite (332 mg, 2 mmol) was added. The resulting solution was heated to reflux for 6 h. Diluted hydrochloric acid (1 mL) was added to the solution, and the mixture was heated for 3 h and cooled down to room temperature. Potassium hydroxide solution (2%) was added to the mixture to pH 10−12. The organic layer was separated, and the aqueous solution was extracted with ethyl acetate (3 × 5 mL). The combined organic layers were washed with water (3 × 10 mL), concentrated potassium carbonate solution (10 mL), dried with sodium sulfate, and evaporated to dryness. The residue was subjected to flash column chromatography (silica gel), eluting with chloroform, to get unreacted **25**, and then with 15% methanol in chloroform to obtain a solid poduct. The product was redissolved in chloroform (5 mL), and HCl solution in methanol (1 mL) was added. The resulting solution was evaporated to dryness to obtain **32** as a purple solid (69 mg, 18%): mp 298−300 °C (dec). IR (KBr) 1703, 1658, 1617, 1570, 1555, 1516 cm^{-1}; ^1H NMR (DMSO-d_6) δ 8.60 (dd, J = 5.4, 1.5 Hz, 1 H), 7.95 (s, 1 H), 7.87 (dd, J = 7.5, 1.5 Hz, 1 H), 7.75 (s, 1 H), 7.59 (s, 1 H), 7.41 (dd, J = 7.5, 5.4 Hz, 1 H), 4.89 (t, J = 6.3 Hz, 2 H), 3.94 (s, 3 H), 3.89 (s, 3 H), 2.88 (t, J = 7.2 Hz, 2 H), 2.42 (s, 3 H), 2.08 (quint, J = 7.0 Hz, 2 H); positive ESIMS m/z (rel intensity) 349 (100), 366 (MH^+, 72). Anal. Calcd for $C_{20}H_{19}N_3O_4 \cdot HCl \cdot 0.6H_2O$: C, 58.22; H, 4.96; N, 9.95. Found: C, 58.21; H, 5.18; N, 10.18.

Topoisomerase I Mediated DNA Cleavage Reactions. Human recombinant Top1 was purified from baculovirus as previously described.[40] DNA cleavage reactions were prepared as previously reported with the exception of the DNA substrate.[25] Briefly, a 117-bp DNA oligonucleotide (Integrated DNA Technologies) encompassing the previously identified Top1 cleavage sites in the 161-bp fragment from pBluescript SK(−) phagemid DNA was employed. This 117-bp oligonucleotide contains a single 5′-cytosine overhang, which was 3′-end-labeled by fill-in reaction with [α-^{32}P]dGTP in React 2 buffer (50 mM Tris-HCl, pH 8.0, 100 mM $MgCl_2$, 50 mM NaCl) with 0.5 unit of DNA polymerase I (Klenow fragment, New England BioLabs). Unincorporated [^{32}P]dGTP was removed using mini Quick Spin DNA columns (Roche, Indianapolis, IN), and the eluate containing the 3′-end-labeled DNA substrate was collected. Approximately 2 nM radiolabeled DNA substrate was incubated with recombinant Top1 in 20 μL of reaction buffer [10 mM Tris-HCl (pH 7.5), 50 mM KCl, 5 mM $MgCl_2$, 0.1 mM EDTA, and 15 μg/mL BSA] at 25 °C for 20 min in the presence of various concentrations of compounds. The reactions were terminated by adding SDS (0.5% final concentration) followed by the addition of two volumes of loading dye (80% formamide, 10 mM sodium hydroxide, 1 mM sodium EDTA, 0.1% xylene cyanol, and 0.1% bromphenol blue). Aliquots of each reaction mixture were subjected to 20% denaturing PAGE. Gels were dried and visualized by using a phosphoimager and ImageQuant software (Molecular Dynamics). For simplicity, cleavage sites were numbered as previously described in the 161-bp fragment.[40]

DNA Unwinding Reactions. These assays were performed in two steps as described.[31] First, SV40 DNA was reacted with excess Top1 for 15 min at 37 °C in the absence of drug to fully relax the DNA. Second, the relaxed DNA was further incubated for 30 min at 37 °C in the presence of increasing (1, 3, 10, 30, 100 μM) concentrations of drugs.

Determination of Drug Water Solubility. Water solubility for **18**, **19**, **33**, or **34** was determined by HPLC according to a previously published protocol.[32] Solid samples of **18**, **19**, **33**, or **34** (4−10 mg) were weighed and added to 1 M Tris buffer solution (250 μL, pH 7.5). The suspensions were shaken for 24 h at 25 °C and then centrifuged, and the supernatants were filtered. Aliquots (10 μL) of the supernatants were injected into the HPLC system equipped with a C18 reverse-phase column (5 μm, 100 Å, 15 cm × 4.6 cm, ES Industries, West Berlin, NJ), eluting with methanol (1% trifluoroacetic acid)/water [90:10 (v:v)]. One point calibration was done by injecting 10 μL aliquots of the corresponding buffer solutions of **18**, **19**, **33**, or **34** with known concentrations.

Quantum Mechanics Calculations. All calculations were performed in Gaussian 09. The structures of model indenoisoquinoline and the A−T and G−C base pairs from models **A** and **B** were optimized at the HF/6-31G** level of theory. The single point energy calculation was performed at the MP2/6-31G* and HF/6-31G* levels of theory. The NBO analysis was performed at HF/6-31G** level of theory.

AUTHOR INFORMATION

Corresponding Author

*Phone: 765-494-1465. Fax: 765-494-6790. E-mail: cushman@purdue.edu.

ACKNOWLEDGMENT

This work was made possible by the National Institutes of Health (NIH) through support of this work with Research Grant UO1 CA89566, as well as through support by the Intramural

Program of the National Cancer Institute, Center for Cancer Research.

■ ABBREVIATIONS USED

AIBN, azobisisobutyronitrile; DIAD, diisopropyl azodicarboxylate; DMF, dimethylformamide; DMSO-d_6, dimethyl-d_6 sulfoxide; NBS, *N*-bromosuccinimide; THF, tetrahydrofuran; Top1, topoisomerase type I; Top1-DNAcc, topoisomerase type I—DNA cleavage complex

■ REFERENCES

(1) Pommier, Y. Topoisomerase I Inhibitors: Camptothecins and Beyond. *Nat. Rev. Cancer* **2006**, *6*, 789–802.

(2) Pommier, Y.; Pourquier, P.; Fan, Y.; Strumberg, D. Mechanism of Action of Eukaryotic DNA Topoisomerase I and Drugs Targeted to the Enzyme. *Biochim. Biophys. Acta, Gene Struct. Expression* **1998**, *1400*, 83–106.

(3) Koster, D. A.; Croquette, V.; Dekker, C.; Shuman, S.; Dekker, N. H. Friction and Torque Govern the Relaxation of DNA Supercoils by Eukaryotic Topoisomerase Ib. *Nature* **2005**, *434*, 671–674.

(4) Redinbo, M. R.; Stewart, L.; Kuhn, P.; Champoux, J. J.; Hol, W. G. J. Crystal Structures of Human Topoisomerase I in Covalent and Noncovalent Complexes with DNA. *Science* **1998**, *279*, 1504–1513.

(5) Wall, M. E.; Wani, M. C.; Cook, C. E.; Palmer, K. H.; Mcphail, A. T.; Sim, G. A. Plant Antitumor Agents. I. Isolation and Structure of Camptothecin a Novel Alkaloidal Leukemia and Tumor Inhibitor from Camptotheca Acuminata. *J. Am. Chem. Soc.* **1966**, *88*, 3888–3890.

(6) Kohn, K. W.; Pommier, Y. Molecular and Biological Determinants of the Cytotoxic Actions of Camptothecins: Perspective for the Development of New Topoisomerase I Inhibitors of Article. *Ann. N.Y. Acad. Sci.* **2000**, *922*, 11–26.

(7) Staker, B. L.; Feese, M. D.; Cushman, M.; Pommier, Y.; Zembower, D.; Stewart, L.; Burgin, A. B. Structures of Three Classes of Anticancer Agents Bound to the Human Topoisomerase I—DNA Covalent Complex. *J. Med. Chem.* **2005**, *48*, 2336–2345.

(8) Cushman, M.; Cheng, L. Stereoselective Oxidation by Thionyl Chloride Leading to Indeno[1,2-*c*]isoquinoline System. *J. Org. Chem.* **1978**, *43*, 3781–3783.

(9) Cushman, M.; Cheng, L. Total Synthesis of Nitidine Chloride. *J. Org. Chem.* **1978**, *43*, 286–288.

(10) Kohlhagen, G.; Paull, K. D.; Cushman, M.; Nagafuji, P.; Pommier, Y. Protein-Linked DNA Strand Breaks Induced by NSC 314622, a Novel Noncamptothecin Topoisomerase I Poison. *Mol. Pharmacol.* **1998**, *54*, 50–58.

(11) Cushman, M.; Jayaraman, M.; Vroman, J. A.; Fukunaga, A. K.; Fox, B. M.; Kohlhagen, G.; Strumberg, D.; Pommier, Y. Synthesis of New Indeno[1,2-*c*]isoquinolines: Cytotoxic Non-Camptothecin Topoisomerase I Inhibitors. *J. Med. Chem.* **2000**, *43*, 3688–3698.

(12) Morrell, A.; Antony, S.; Kohlhagen, G.; Pommier, Y.; Cushman, M. A Systematic Study of Nitrated Indenoisoquinolines Reveals a Potent Topoisomerase I Inhibitor. *J. Med. Chem.* **2006**, *49*, 7740–7753.

(13) Antony, S.; Agama, K. K.; Miao, Z. H.; Takagi, K.; Wright, M. H.; Robles, A. I.; Varticovski, L.; Nagarajan, M.; Morrell, A.; Cushman, M.; Pommier, Y. Novel Indenoisoquinolines NSC 725776 and NSC 724998 Produce Persistent TopoIsomerase I Cleavage Complexes and Overcome Multidrug Resistance. *Cancer Res.* **2007**, *67*, 10397–10405.

(14) Pommier, Y.; Cushman, M. The Indenoisoquinoline Noncamptothecin Topoisomerase I Inhibitors: Update and Perspectives. *Mol. Cancer Ther.* **2009**, *8*, 1008–1014.

(15) Clinical Study: 10-C-0056, a Phase I Study of Indenoisoquinolines LMP400 and LMP776 in Adults with Relapsed Solid Tumors and Lymphomas. http://clinicalstudies.info.nih.gov/cgi/detail.cgi?A_2010-C-0056.html (accessed July 2011).

(16) Morrell, A.; Placzek, M. S.; Steffen, J. D.; Antony, S.; Agama, K.; Pommier, Y.; Cushman, M. Investigation of the Lactam Side Chain Length Necessary for Optimal Indenoisoquinoline Topoisomerase I Inhibition and Cytotoxicity in Human Cancer Cell Cultures. *J. Med. Chem.* **2007**, *50*, 2040–2048.

(17) Nagarajan, M.; Morrell, A.; Ioanoviciu, A.; Antony, S.; Kohlhagen, G.; Agama, K.; Hollingshead, M.; Pommier, Y.; Cushman, M. Synthesis and Evaluation of Indenoisoquinoline Topoisomerase I Inhibitors Substituted with Nitrogen Heterocycles. *J. Med. Chem.* **2006**, *49*, 6283–6289.

(18) Nagarajan, M.; Xiao, X. S.; Antony, S.; Kohlhagen, G.; Pommier, Y.; Cushman, M. Design, Synthesis, and Biological Evaluation of Indenoisoquinoline Topoisomerase I Inhibitors Featuring Polyamine Side Chains on the Lactam Nitrogen. *J. Med. Chem.* **2003**, *46*, 5712–5724.

(19) Morrell, A.; Placzek, M.; Parmley, S.; Antony, S.; Dexheimer, T. S.; Pommier, Y.; Cushman, M. Nitrated Indenoisoquinolines as Topoisomerase I Inhibitors: A Systematic Study and Optimization. *J. Med. Chem.* **2007**, *50*, 4419–4430.

(20) Morrell, A.; Placzek, M.; Parmley, S.; Grella, B.; Antony, S.; Pommier, Y.; Cushman, M. Optimization of the Indenone Ring of Indenoisoquinoline Topoisomerase I Inhibitors. *J. Med. Chem.* **2007**, *50*, 4388–4404.

(21) Dillow, G. W.; Kebarle, P. Electron-Affinities of Aza-Substituted Polycyclic Aromatic-Hydrocarbons. *Can. J. Chem.* **1989**, *67*, 1628–1631.

(22) Jagtap, P. G.; Baloglu, E.; Southan, G.; Williams, W.; Roy, A.; Nivorozhkin, A.; Landrau, N.; Desisto, K.; Salzman, A. L.; Szabo, C. Facile and Convenient Syntheses of 6,11-Dihydro-5*H*-indeno[1,2-*c*]-isoquinolin-5-ones and 6,11-Dihydro-5*H*-indolo[3,2-*c*]isoquinolin-5-one. *Org. Lett.* **2005**, *7*, 1753–1756.

(23) Potts, K. T.; Robinson, R. Synthetical Experiments Related to the Indole Alkaloids. *J. Chem. Soc.* **1955**, 2675–2686.

(24) Whitmore, W. F.; Cooney, R. C. The Preparation of Homophthalyl Cyclic Hydrazide and 4-Aminohomophthalyl Cyclic Hydrazide. *J. Am. Chem. Soc.* **1944**, *66*, 1237–1240.

(25) Dexheimer, T. S.; Pommier, Y. DNA Cleavage Assay for the Identification of Topoisomerase I Inhibitors. *Nat. Protoc.* **2008**, *3*, 1736–1750.

(26) Boyd, M. R.; Pauli, K. D. Some Practical Considerations and Applications of the National-Cancer-Institute in-Vitro Anticancer Drug Discovery Screen. *Drug Dev. Res.* **1995**, *34*, 91–109.

(27) Skehan, P.; Storeng, R.; Scudiero, D.; Monks, A.; Mcmahon, J.; Vistica, D.; Warren, J. T.; Bokesch, H.; Kenney, S.; Boyd, M. R. New Colorimetric Cytotoxicity Assay for Anticancer-Drug Screening. *J. Natl. Cancer Inst.* **1990**, *82*, 1107–1112.

(28) Skehan, P.; Storeng, R.; Scudiero, D.; Monks, A.; McMahon, J.; Vistica, D.; Warren, J. T.; Bokesch, H.; Kenney, S.; Boyd, M. R. New Colorimetric Cytotoxicity Assay for Anticancer-Drug Screening. *J. Natl. Cancer Inst.* **1990**, *82*, 1107–1112.

(29) Boyd, M. R.; Paull, K. D. Some Practical Considerations and Applications of the National Cancer Institute in Vitro Anticancer Drug Discovery Screen. *Drug Dev. Res.* **1995**, *34*, 91–109.

(30) Morrell, A.; Antony, S.; Kohlhagen, G.; Pommier, Y.; Cushman, M. Synthesis of Benz[*d*]indeno[1,2-*b*]pyran-5,11-diones: Versatile Intermediates for the Design and Synthesis of Topoisomerase I Inhibitors. *Bioorg. Med. Chem. Lett.* **2006**, *16*, 1846–1849.

(31) Pommier, Y.; Covey, J. M.; Kerrigan, D.; Markovits, J.; Pham, R. DNA Unwinding and Inhibition of Mouse Leukemia-L1210 DNA Topoisomerase-I by Intercalators. *Nucleic Acids Res.* **1987**, *15*, 6713–6731.

(32) Vogel, G. H. Determination of Solubility by Hyphenated HPLC Methods. In *Drug Discovery and Evaluation: Safety and Pharmacokinetiks Assay*; Springer: New York, 2006; pp 400—402.

(33) Cheng, K. J.; Rahier, N. J.; Eisenhauer, B. M.; Gao, R.; Thomas, S. J.; Hecht, S. M. 14-Azacamptothecin: A Potent Water-Soluble Topoisomerase I Poison. *J. Am. Chem. Soc.* **2005**, *127*, 838–839.

(34) Rahier, N. J.; Cheng, K. J.; Gao, R.; Eisenhauer, B. M.; Hecht, S. M. Synthesis of 14-Azacamptothecin, a Water-Soluble Topoisomerase I Poison. *Org. Lett.* **2005**, *7*, 835–837.

(35) Song, Y. L.; Cushman, M. The Binding Orientation of a Norindenoisoquinoline in the Topoisomerase I—DNA Cleavage Complex Is Primarily Governed by Pi—Pi Stacking Interactions. *J. Phys. Chem. B* **2008**, *112*, 9484–9489.

(36) Xiao, X. S.; Antony, S.; Pommier, Y.; Cushman, M. On the Binding of Indeno[1,2-*c*]isoquinolines in the DNA−Topoisomerase I Cleavage Complex. *J. Med. Chem.* **2005**, *48*, 3231–3238.

(37) Xiao, X. S.; Cushman, M. An Ab Initio Quantum Mechanics Calculation That Correlates with Ligand Orientation and DNA Cleavage Site Selectivity in Camptothecin−DNA−Topoisomerase I Ternary Cleavage Complexes. *J. Am. Chem. Soc.* **2005**, *127*, 9960–9961.

(38) Frisch, M. J.; Trucks, G. W.; Schlegel, H. B.; Scuseria, G. E.; Robb, M. A.; Cheeseman, J. R.; Scalmani, G.; Barone, V.; Mennucci, B.; Petersson, G. A.; Nakatsuji, H.; Caricato, M.; Li, X.; Hratchian, H. P.; Izmaylov, A. F.; Bloino, J.; Zheng, G.; Sonnenberg, J. L.; Hada, M.; Ehara, M.; Toyota, K.; Fukuda, R.; Hasegawa, J.; Ishida, M.; Nakajima, T.; Honda, Y.; Kitao, O.; Nakai, H.; Vreven, T.; Montgomery, J. A., Jr.; Peralta, J. E.; Ogliaro, F.; Bearpark, M.; Heyd, J. J.; Brothers, E.; Kudin, K. N.; Staroverov, V. N.; Kobayashi, R.; Normand, J.; Raghavachari, K.; Rendell, A.; Burant, J. C.; Iyengar, S. S.; Tomasi, J.; Cossi, M.; Rega, N.; Millam, J. M.; Klene, M.; Knox, J. E.; Cross, J. B.; Bakken, V.; Adamo, C.; Jaramillo, J.; Gomperts, R.; Stratmann, R. E.; Yazyev, O.; Austin, A. J.; Cammi, R.; Pomelli, C.; Ochterski, J. W.; Martin, R. L.; Morokuma, K.; Zakrzewski, V. G.; Voth, G. A.; Salvador, P.; Dannenberg, J. J.; Dapprich, S.; Daniels, A. D.; Farkas; Foresman, J. B.; Ortiz, J. V.; Cioslowski, J.; Fox, D. J. *Gaussian 09*, revision A.02; Gaussian, Inc.: Wallingford, CT, 2009.

(39) Glendening, E. D.; Reed, A. E.; Carpenter, J. E.; Weinhold, F. *NBO*, version 3.1.

(40) Pourquier, P.; Ueng, L. M.; Fertala, J.; Wang, D.; Park, H. J.; Essigmann, J. M.; Bjornsti, M. A.; Pommier, Y. Induction of Reversible Complexes between Eukaryotic DNA Topoisomerase I and DNA-Containing Oxidative Base Damages—7,8-Dihydro-8-oxoguanine and 5-Hydroxycytosine. *J. Biol. Chem.* **1999**, *274*, 8516–8523.